ORIGINAL ARTICLE

RECORDS OF PHARMACEUTICAL AND BIOMEDICAL SCIENCES

Diallyl Disulfide Ameliorates Kidney Damage Associated with Polycystic Ovary Syndrome by Targeting STAT1/ NF-κB and Nrf2/HO-1 Signaling

Hala I. Madkour[1], Reda S. Yousef [2], Rasha Mokhtar Abdelkareem[3], Eman Mohammed Ali[1]*

[1] Department of Clinical Pharmacology, Faculty of Medicine, Sohag University, Egypt; [2] Department of Biochemistry, Faculty of Medicine, Sohag University, Egypt;[3] Department of Pathology, Faculty of Medicine, Sohag University, Egypt.

Received: 04. 8. 2024

Revised: 20. 8. 2024

Accepted: 23. 8. 2024

*Correspondence Author:

E-mail address:

emanmohamed@med.sohag.edu.eg

Abstract

Diallyl disulfide (DADS), a significant bioactive component of garlic, has many advantageous biological purposes. It is unknown how DADS affects renal disorder in PCOS patients. In a rat model of PCOS, our study postulated that DADS would safeguard against renal dysfunction possibly by combating NF-κB and enhancing Nrf2 dependent mechanism. Female Wistar rats were randomly divided into 4 groups (n = 8); normal control, PCO induced by letrozole (LET) (1 mg $kg^{-1}day^{-1}$, p.o.), protective group; DADS (50 mg kg^{-1} day^{-1}, p.o.) + LET, and therapeutic group; LET followed by DADS treatment. DADS significantly reduced serum creatinine, urea, body weight, hyperinsulinemia, hyperglycemia, hyperandrogenism, and dyslipidemia. In addition, DADS obviously diminished PCOS-induced elevations in STAT1, NF-κB, TNFα, and IL6 and increased IL10. Moreover, DADS significantly reduced oxidative stress markers (MDA and NOX4) and increased SOD, GST, and PON1 in renal tissue. Furthermore, DADS positively regulated the Nrf2, HO-1, and NQO1 genes. DADS up-regulates Bcl2 expression in cortical glomerular capillaries and renal tubules and downregulates the expression of caspase-3. Our research revealed that DADS significantly ameliorated kidney dysfunction and renal injury associated with PCOS. The antioxidant, anti-inflammatory, and anti-apoptotic properties of DADS may signify a crucial part of its applications in therapy. DADS may be a probable therapy in PCOS to lessen the linked kidney damage through targeting STAT1/ NF-κB and Nrf2/HO-1 signaling.

Keywords: Diallyl disulfide; polycystic ovary syndrome; Bcl2/caspase-3, STAT1/NF-κB; Nrf2/HO-1; renal dysfunction.

1. Introduction

Polycystic ovary syndrome (PCOS) is one of the most common endocrine diseases affecting women of reproductive age **(Escobar-Morreale, 2018)**. Oligomenorrhea, irregular ovulation, polycystic ovarian morphology **(Azziz et al., 2016)**, and a number of metabolic disorders like hyperandrogenism, hyperinsulinemia, and dyslipidemia are characteristics of PCOS **(Goodarzi et al., 2011)**. Additionally, PCOS is associated with numerous systemic complications

(Behboudi-Gandevani et al., 2020). Strong correlations have been found between PCOS and obesity, hyperlipidemia, fatty liver, type 2 diabetes, hypertension, anxiety, depression **(Cooney et al., 2017)**, endometrial cancer, and cardiovascular diseases **(Cooney and Dokras, 2018)**.

Chronic kidney disease (CKD) is a gradual decline of renal function over time. It can progress to end-stage kidney failure and uremia, with a significantly higher death rate if lacking early prevention, management, and treatment **(Nigam and Bush, 2019)**. Metabolic syndrome characteristics, in particular, diabetes, obesity, and cardiovascular disease are strongly correlated with CKD mortality rates **(Chadban et al., 2010; Piccoli et al., 2018)**. As previously stated, PCOS patients are associated with a number of metabolic disorders, and this results in the development of further chronic illnesses. PCOS and CKD are causally linked **(Du et al., 2023)**. Many studies demonstrated that PCOS triggers CKD due to metabolically connected elements like obesity and abnormal hormone secretion **(Patil et al., 2017; Behboudi-Gandevani et al., 2020)**.

Garlic contains a naturally occurring organic compound called diallyl disulfide (DADS), which has antioxidant and anti-inflammatory properties. **(Lee et al., 2014)**. Reports are stating that DADS prevents renal injury caused by acetaminophen and glycerol in rodents, mostly due to its antioxidant and anti-inflammatory characteristics **(Ko et al., 2017; Sharma et al., 2021)**. The use of herbal medicines has always been considered. It is interesting to note that natural substances may offer a novel and promising approach with greater efficacy and less toxicity. The purpose of this research was to explore the probable protective and therapeutic effect of DADS versus kidney injury accompanying PCOS in rats and the potential mechanism of DADS in improving kidney dysfunction.

2. Materials and Methods

2.1. Drugs and Chemicals

Diallyl disulfide and letrozole (LET) were procured from Sigma Aldrich Co, (England). Dimethyl sulfoxide (DMSO) was obtained from GFS chemicals Co, (India).

Superoxide dismutase (SOD) (Cat. No. SD 25 21), Glutathione-S-transferase (GST) (Cat. No. GT 25 19), and malondialdehyde (MDA) (Cat. No. MD 25 29) were procured from the Bio-diagnostic Co, (Egypt). From Bioassay technology laboratory (Shanghai. China), kits for assay of paraoxonase-1 (PON1) (Cat. No. E0867Ra) and nicotinamide adenine dinucleotide phosphate oxidase 4 (NADPH Oxidase 4) (NOX4) (Cat. No. E1298Ra) were bought.

Kits for estimation of tumor necrosis factor α (TNFα) (Cat. No. E-EL-R0019) and interleukin 6 (IL6) (Cat. No. E-EL-R0015) were obtained from Elabscience Biotechnology Inc. (USA). Interleukin 10 (IL10) (Cat. No. CSB-E04595r) and nuclear factor-κB (NF-κB) (Cat. No. CSB-E13148r) detection kits were taken from Cusabio Technology LLC (USA). ELK Biotechnology Co., LTD (USA) provided signal transducer and activator of transcription 1 (STAT1) (Cat. No. ELK8989) detection kits.

Urea (Cat. No. 1001332) and creatinine (Cat. No. 1001115) assay kits were purchased from Spinreact Co. (Spain). Kits for the detection of testosterone (Cat. No. E0259Ra) and insulin (Cat. No. E0707Ra) were purchased from the Bioassay technology laboratory (Shanghai, China). Bio-diagnostic Company (Egypt) provided kits for glucose (Cat. No. GL 13 20). Total cholesterol (TC), triglycerides (TG), and high-density lipoprotein (HDL) were detected using kits from Human Gesellschaft Für Biochemica and Diagnostica mbH (Wiesbaden, Germany).

2.2. Animals

A total of 32 prepubertal female Wistar rats, 4 weeks old, with average body weight of 95±5 g taken from the animal house, Faculty of Medicine, Sohag University, Egypt, were used in the experiment. Rats were housed under standardized conditions (normal light/dark cycles, temperature of 22±2°C, and 50±10% humidity). The rats were allowed to have unrestricted access to water and food. The European Union Guidelines for the Care and Use of Laboratory Animals (European Union Directive 2010/63/EU) were strictly followed throughout the entire study process, and it was authorized by the Institutional Animal Care and Use Committee of Sohag University, Faculty of Medicine, Sohag, Egypt (Approval No. Sohag-5-5-1/2024-01).

2.3. Experimental design

The animals were split into four groups at random with eight animals each, after acclimatization for a week.

Control group: rats were administered DMSO (0.5%) orally daily for the entire period of the experiment.

PCOS group: rats received LET (1 mg kg^{-1} day^{-1} p.o) **(Olaniyi et al., 2021)** for 5 weeks to develop PCOS. Manifestation of PCOS was verified by tracking testosterone levels and performing histopathology of the ovaries.

PCOS+DADS pre-treatment group (protective): rats were given DADS (50 mg kg^{-1} day^{-1} p.o) **(Somade et al., 2019)** 1 hour before LET (1 mg kg^{-1} day^{-1} p.o) for 5 weeks.

PCOS+DADS post-treatment group (therapeutic): rats were given LET (1 mg kg^{-1} day^{-1} p.o) for 5 weeks and then DADS (50 mg kg^{-1} day^{-1} p.o) was administered for 5 weeks after induction of PCOS.

2.4. Sample collection

At the end of the experiment, all rats were weighed and then they had isoflurane anesthesia. Blood samples were collected by heart puncture, serum was extracted and kept frozen for estimation of kidney function biomarkers, testosterone, insulin, glucose, and lipid profile. After that, animals were sacrificed via cervical dislocation to separate tissue samples. Ovaries and kidneys were removed carefully from each animal. The right ovary and the right kidney were immediately fixed in 10% formalin. Confirmation of PCOS development in the ovary was done. Histopathological changes and expression of apoptotic markers by immunohistochemistry were evaluated in the kidney. The left kidney was divided into two divisions; one was immediately frozen in liquid nitrogen and preserved at -80 °C for real-time quantitative polymerase chain reaction (RT q-PCR) analysis. The second was rinsed in ice-cold water, weighed, and homogenized in phosphate-buffered saline (pH 7.4). The tissue homogenate was centrifuged at 4000 rpm for 15 min, after which the supernatant was removed and kept at -80°C till the biochemical assay.

2.5. Calculation of body weight

Animal body weight was measured by placing the animal on a weighing scale. Animals were weighed both before and after the experiment, and the final body weight was calculated.

2.6. Biochemical analysis

2.6.1. Determination of serum testosterone, insulin, and glucose levels

Testosterone and insulin were estimated using enzyme-linked immunosorbent assay (ELISA) according to the recommendations of the manufacturer. Testosterone was indicated as nmol L^{-1} whereas insulin was expressed as mIU L^{-1}. Glucose was assayed spectrophotometrically (Photometer 5010, Germany) and was reported as mg dL^{-1}.

2.6.2. Determination of lipid profile

Total cholesterol, TG, and HDL were assayed spectrophotometrically (photometer 5010, Germany), whereas Friedewald's Formula was employed to estimate LDL **(Friedewald et al., 1972)**:

LDL-C=TC - HDL-C - TG/5

2.6.3. Determination of kidney function biomarkers

Urea and creatinine were estimated spectrophotometrically (Photometer 5010, Germany).

2.6.4. Determination of renal antioxidant/oxidant status

Superoxide dismutase and GST were measured based on the procedure of **Nishikimi et al. (1972)** and **Habig et al. (1974)**, respectively by a colorimetric technique. The levels of SOD and GST were reported as U g^{-1} tissue. Lipid peroxidation was assayed by the measurement of MDA levels colorimetrically as stated by **Ohkawa et al. (1979)** approach. Values were presented as nmol g^{-1} tissue. PON1 and NOX4 were assayed by ELISA in accordance with the manufacturer's rules and their levels were depicted as ng g^{-1} tissue.

2.6.5. Determination of renal inflammatory markers and transcription factors

Using ELISA, the levels of inflammatory markers (TNFα, IL6, IL10) and transcription factors (NF-κB and STAT1) were assayed in line with the manufacturer's protocol. TNFα, IL6, IL10, and NF-κB levels were presented as pg g^{-1} tissue whereas STAT1 was recorded as ng g^{-1} tissue.

2.7. Real-time q-PCR analysis

Total RNA was taken out from the kidney tissue using TRI REAGENT (Bioshop Co, Canada) following the manufacturer's rules. A one-step reaction was applied to reverse transcribe mRNA into cDNA. The real-time PCR assay uses RNA as a template, and reverse transcription takes place while the assay is running. To amplify a segment of the target cDNA, modified gene-specific PCR primers (Metabione Co, Germany) are utilized following the reaction in real-time. The steps were performed using a GoTaqR 1-Step RT-qPCR System (Promega Company, USA) on a real-time PCR machine (applied biosystems step one plus). The following parameters were used in quantitative PCR for several cycles: denaturation at 95 °C for 10 s, annealing at 60 °C for 30 s, and extension at 72 °C for 30 s. The comparative approach, $^{2-\Delta\Delta}$CT was utilized to determine the relative expression level of every gene, normalized to the expression levels of GAPDH **(Livak and Schmittgen, 2001)**. **Table 1** shows the primers.

2.8. Histological and immunohistochemical studies

The kidney and ovary specimens that had been preserved in formalin underwent the following processing for histological and immunohistochemical analyses.

2.8.1. Histological investigation

Formalin-fixed ovary and kidney tissues were gathered. Hematoxylin and eosin (H&E)-stained sections of 5 µm thickness were made and examined under a light microscope.

2.8.2. Immunohistochemical Staining

Immunohistochemistry of Bcl2 and caspase-3 antibodies carried out using avidin biotin peroxidase complex method. The chosen paraffin blocks were divided into 4µm thick sections, which were deparaffinized and rehydrated, followed by a distilled water rinse. Tissue sections were incubated in 0.6% hydrogen peroxide to block endogenous peroxidase activity. Sections were then incubated with rabbit anti-human Bcl2 antibody (clone EP36, Cat. # AN723-5M, BioGenex) and polyclonal anti-cleaved-caspase-3 rabbit antibodies (clone P70677, Cat. #GB11532). After that, slides were incubated with a goat anti-rabbit secondary antibody for 30 min after being washed by phosphate-buffered saline. DAB kit was used for staining tissue sections before being counter-stained with Mayer's hematoxylin. The immunostaining interpretation of Bcl2 and caspase-3 was done using light microscopy.

Table 1. The sets of primers used in real-time q-PCR analysis

Target genes	Direction and sequence
Nrf2	**F**: 5′-CACATCCAGACAGACACCAGT-3′ **R**: 5′-CTACAAATGGGAATGTCTCTGC-3′
HO-1	**F**: 5′-ACAGGGTGACAGAAGAGGCTAA-3′ **R**: 5′-CTGTGAGGGACTCTGGTCTTTGG-3′
NQO1	**F**: 5′-CAGCGGCTCCATGTACT-3′ **R**: 5′-GACCTGGAAGCCACAGAAG-3′
GAPDH	**F**: 5′-AGGTTGTCTCCTGTGACTTC-3′ **R**: 5′-CTGTTGCTGTAGCCATATTC-3′

Nrf2= Nuclear factor erythroid 2-related factor 2, HO-1= Heme oxygenase-1, NQO1= NADPH quinone oxidoreductase 1.

2.9. Statistical analysis

Data were indicated as mean ± SE. The one-way analysis of variance (ANOVA) was used to analyze all data using the SPSS program (Statistical Package for the Social Sciences, version 25.0, SPSS Inc, Chicago, IL, USA). Tukey's post hoc test was utilized to compare the groups' means. $p<0.05$ was deemed significant.

3. Results

3.1. Effect of DADS on body weight in LET-induced PCOS

The body weight of rats was determined before and after the experiment as the increase in body weight is one of the most important clinical characteristics of PCOS. Our results exhibited a significant rise ($p<0.05$) in body weight in PCOS animals compared to normal controls, which was thereafter reversed ($p<0.05$) in PCOS animals administered DADS pre- and post-treatment when compared with PCOS group. Furthermore, a considerable decrease in body weight ($p<0.05$) occurred in DADS pre-treatment group compared to DADS post-treatment group **(Fig. 1)**.

3.2. Hormonal evidence of PCOS induction and effect of DADS on serum testosterone level in LET-induced PCOS

A significant rise ($p<0.05$) in serum testosterone level was observed in PCOS rats when compared with the control rats. However, pre- and post-treatment with DADS produced a remarkable decrease ($p<0.05$) in serum testosterone level compared to PCOS group **(Fig. 2)**.

3.3. Effect of DADS on serum insulin and glucose levels in LET-induced PCOS

The results demonstrated in **Table 2** show that serum insulin and glucose levels in PCOS rats were significantly higher ($p<0.05$) than in the control group. In contrast, pre- and post-treatment with DADS caused a remarkable reduction ($p<0.05$) in both parameters compared to PCOS rats.

3.4. Effect of DADS on lipid profile in LET-induced PCOS

Table 3 proves that there was a significant rise ($p<0.05$) in TC, TG, and LDL and a significant reduction ($p<0.05$) in HDL in animals with PCOS compared to the control group. However, TC, TG, and LDL were reduced ($p<0.05$) and HDL was elevated upon pre- and post-treatment with DADS when compared with PCOS group.

3.5. Effect of DADS on kidney function biomarkers in LET-induced PCOS

Comparing the PCOS group to the control rats, **Table 4** reveals a significant ($p<0.05$) rise in serum urea and creatinine. While DADS pre- and post-treatment data showed a significant decline ($p<0.05$) in these indicators compared to PCOS animals. Moreover, DADS pre-treatment group displayed a substantial decline ($p<0.05$) in the kidney function biomarkers compared to DADS post-treatment group.

3.6. Effect of DADS on renal antioxidant/oxidant status in LET-induced PCOS

3.6.1. Antioxidant biomarkers

Table 5 presents significantly decreased ($p<0.05$) levels of renal SOD, GST and PON1 in PCOS group compared to the control rats. Instead, DADS pre- and post-treatment showed a significant elevation ($p<0.05$) in the previous parameters compared to PCOS group. In addition, there was a significant elevation ($p<0.05$) in SOD, GST, and PON1 levels in DADS pre-treatment group compared to DADS post-treatment group.

3.6.2. Oxidative biomarkers

There was a significant rise ($p<0.05$) in renal MDA and NOX4 levels in PCOS group compared to the control group. In contrast, as compared to the PCOS group, pre- or post-treatment with DADS was associated with a significant ($p< 0.05$) decline in MDA and NOX4. Moreover, DADS pre-treatment group exhibited a significant reduction ($p<0.05$) in the levels of MDA and NOX4 compared to DADS post-treatment group **(Fig. 3 and 4)**.

3.7. Effect of DADS on renal inflammatory markers and transcription factors in LET-induced PCOS

Table 6 displays a significant rise ($p<0.05$) in TNFα, IL6, NF-κB, and STAT1 and a considerable

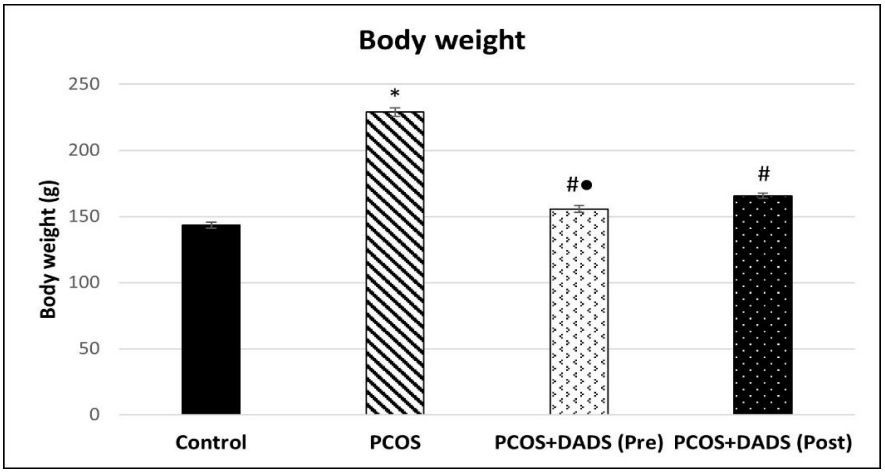

Fig. 1. Effect of DADS (50 mg kg^{-1} day^{-1}, p.o.) on body weight in LET (1 mg kg^{-1} day^{-1}, p.o.)-induced PCOS. Data are displayed as mean ± SE (n=8). PCOS=Polycystic ovary syndrome, DADS=Diallyl disulfide. * p<0.05 contrasted with control group, # p<0.05 contrasted with PCOS group, ● p<0.05 contrasted with DADS (post) group.

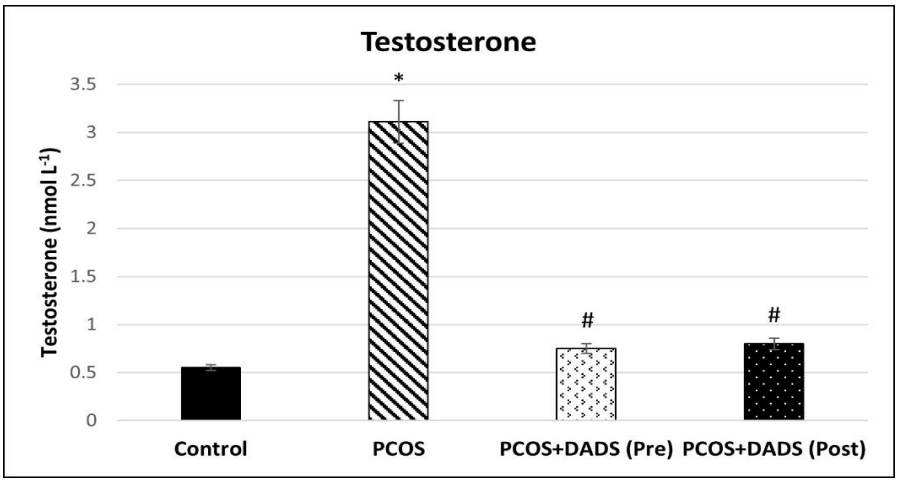

Fig. 2. Effect of DADS (50 mg kg^{-1} day^{-1}, p.o.) on serum testosterone in LET (1 mg kg^{-1} day^{-1}, p.o.)-induced PCOS. Data are displayed as mean ± SE (n=8). PCOS=Polycystic ovary syndrome, DADS=Diallyl disulfide. * p<0.05 contrasted with control group, # p<0.05 contrasted with PCOS group.

Table 2. Effect of DADS (50 mg kg^{-1} day^{-1}, p.o.) on serum insulin and glucose levels in LET (1 mg kg^{-1} day^{-1}, p.o.) induced PCOS

Groups	Insulin (mIU L^{-1})	Glucose (mg dL^{-1})
Control	1.83±0.1	102.82±6.44
PCOS	5.24±0.37*	173.82±5.34*
PCOS+DADS (Pre)	2.25±0.14$^{\#}$	118.44±4.82$^{\#}$
PCOS+DADS (Post)	2.4±0.15$^{\#}$	125.84±3.87$^{\#}$

Data are displayed as mean ± SE (n=8). PCOS=Polycystic ovary syndrome, DADS=Diallyl disulfide. * p<0.05 contrasted with control group, # p<0.05 contrasted with PCOS group.

Table 3. Effect of DADS (50 mg kg^{-1} day^{-1}, p.o.) on lipid profile in LET (1 mg kg^{-1} day^{-1}, p.o.)-induced PCOS

Groups	TC (mg dL^{-1})	TG (mg dL^{-1})	HDL (mg dL^{-1})	LDL (mg dL$^{-1)}$
Control	110.84±4.76	104.7±5.3	55.72±2.34	34.18±2.56
PCOS	202.07±6.63*	203.82±6.34*	27.87±1.23*	133.43±5.66*
PCOS+DADS (Pre)	118.46±3.34$^{\#}$	120.75±2.24$^{\#}$	50.8±2.58$^{\#}$	43.51±3.39$^{\#}$
PCOS+DADS (Post)	122.97±2.23$^{\#}$	123.36±3.64$^{\#}$	45.02±1.64$^{\#}$	53.28±2.79$^{\#}$

Data are displayed as mean ± SE (n=8). PCOS=Polycystic ovary syndrome, DADS=Diallyl disulfide, TC=Total cholesterol, TG=Triglycerides, HDL=High density lipoprotein, LDL= Low density lipoprotein. * p<0.05 contrasted with control group, # p<0.05 contrasted with PCOS group.

Table 4. Effect of DADS (50 mg kg^{-1} day^{-1}, p.o.) on kidney function biomarkers in LET (1 mg kg^{-1} day^{-1}, p.o.)-induced PCOS

Groups	Urea (mg dL^{-1})	Creatinine (mg dL^{-1})
Control	36.52±1.96	0.85±0.03
PCOS	74.72±2.31*	1.87±0.04*
PCOS+DADS (Pre)	33.56±1.82$^{\#\bullet}$	0.87±0.03$^{\#\bullet}$
PCOS+DADS (Post)	55.33±2.32$^{\#}$	1.42±0.04$^{\#}$

Data are displayed as mean ± SE (n=8). PCOS=Polycystic ovary syndrome, DADS=Diallyl disulfide. * p<0.05 contrasted with control group, # p<0.05 contrasted with PCOS group, ● p<0.05 contrasted with DADS (post) group.

Table 5. Effect of DADS (50 mg kg^{-1} day^{-1}, p.o.) on renal antioxidant biomarkers in LET (1 mg kg^{-1} day^{-1}, p.o.)-induced PCOS

Groups	SOD (U g^{-1})	GST (U g^{-1})	PON1 (ng g^{-1})
Control	2.27±0.09	2.39±0.08	18.73±0.52
PCOS	0.98±0.07*	1.07±0.07*	5.21±0.12*
PCOS+DADS (Pre)	2.34±0.05$^{\#\bullet}$	2.41±0.08$^{\#\bullet}$	19.5±0.67$^{\#\bullet}$
PCOS+DADS (Post)	1.73±0.05$^{\#}$	2.05±0.09$^{\#}$	10.68±0.75$^{\#}$

Data are displayed as mean ± SE (n=8). PCOS=Polycystic ovary syndrome, DADS=Diallyl disulfide, SOD=Superoxide dismutase, GST=Glutathione-S-transferase, PON1= Paraoxonase-1. * p<0.05 contrasted with control group, # p<0.05 contrasted with PCOS group, ● p<0.05 contrasted with DADS (post) group.

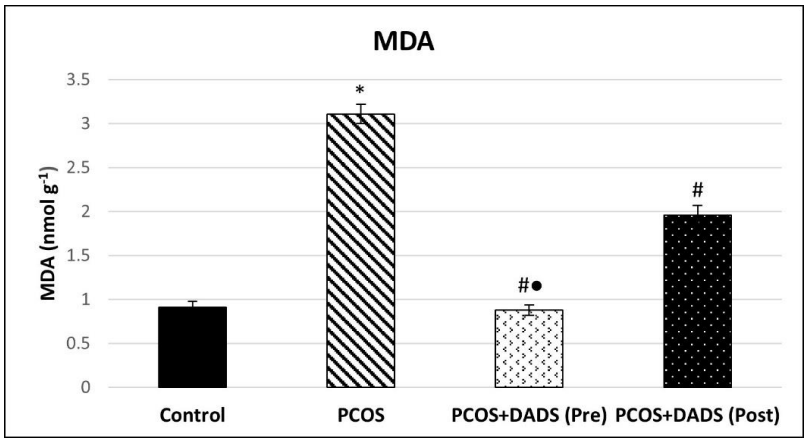

Fig. 3. Effect of DADS (50 mg kg^{-1} day^{-1}, p.o.) on renal MDA in LET (1 mg kg^{-1} day^{-1}, p.o.)-induced PCOS. Data are displayed as mean ± SE (n=8). PCOS=Polycystic ovary syndrome, DADS=Diallyl disulfide, MDA=Malondialdehyde. * p<0.05 contrasted with control group, # p<0.05 contrasted with PCOS group, ● p<0.05 contrasted with DADS (post) group.

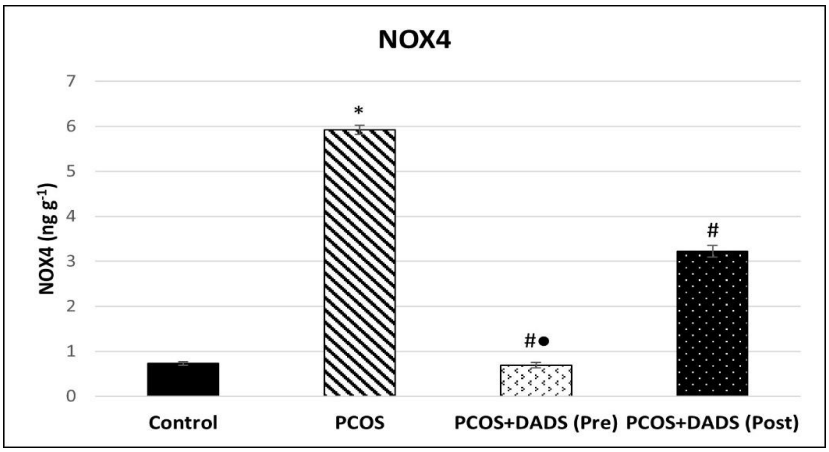

Fig. 4. Effect of DADS (50 mg kg^{-1} day^{-1}, p.o.) on renal NOX4 in LET (1 mg kg^{-1} day^{-1}, p.o.)-induced PCOS. Data are displayed as mean ± SE (n=8). PCOS=Polycystic ovary syndrome, DADS=Diallyl disulfide, NOX4= NADPH Oxidase 4. * p<0.05 contrasted with control group, # p<0.05 contrasted with PCOS group, ● p<0.05 contrasted with DADS (post) group.

Table 6. Effect of DADS (50 mg kg^{-1} day^{-1}, p.o.) on renal inflammatory markers and transcription factors in LET (1 mg kg^{-1} day^{-1}, p.o.)-induced PCOS

Groups	TNFα (pg g^{-1})	IL6 (pg g^{-1})	IL10 (pg g^{-1})	NF-κB (pg g^{-1})	STAT1 (ng g^{-1})
Control	69.89±3.17	12.68±0.58	18.09±0.73	1.65±0.1	0.34±0.02
PCOS	128.77±8.31*	22.29±0.68*	3.58±0.22*	3.14±0.15*	2.87±0.13*
PCOS+DADS (Pre)	71.08±2.96$^{\#\bullet}$	11.53±0.56$^{\#\bullet}$	19.97±0.52$^{\#\bullet}$	1.59±0.1$^{\#\bullet}$	1.33±0.1$^{\#\bullet}$
PCOS+DADS (Post)	98.64±7.86$^{\#}$	17.91±0.67$^{\#}$	10.19±0.46$^{\#}$	2.37±0.13$^{\#}$	1.96±0.11$^{\#}$

Data are displayed as mean ± SE (n=8). PCOS=Polycystic ovary syndrome, DADS=Diallyl disulfide, TNFα=Tumor necrosis factor α, IL6=Interleukin 6, IL10=Interleukin 10, NF-κB= nuclear factor-κB, STAT1=Signal transducer and activator of transcription 1. * p<0.05 contrasted with control group, # p<0.05 contrasted with PCOS group, ● p<0.05 contrasted with DADS (post) group.

reduction (p<0.05) in IL10 in PCOS group compared to the control group. Conversely, there was a significant decline (p<0.05) in TNFα, IL6, NF-κB, and STAT1 and a significant elevation (p<0.05) in IL10 levels in DADS pre- and post-treatment compared to PCOS group. Likewise, there was a significant decline (p<0.05) in TNFα, IL6, NF-κB and STAT1 and a substantial elevation (p<0.05) in IL10 levels in DADS pre-treatment group compared to DADS post-treatment group.

3.8. Effect of DADS on the expression of renal genes Nrf2, HO-1, and NQO1 in LET-induced PCOS

In PCOS group, the levels of mRNA expression of Nrf2, HO-1, and NQO1 genes were downregulated (p<0.05) compared to the control group. Alternatively, there was an upregulation (p<0.05) in their levels in DADS pre- and post-treatment in comparison with the PCOS group. In addition, DADS pre-treatment group presented an upregulation (p<0.05) in the levels of mRNA expression of Nrf2, HO-1, and NQO1 genes compared to DADS post-treatment group **(Fig. 5-7)**.

3.9. Effect of DADS on histological and immunohistochemical studies in LET-induced PCOS

3.9.1. Histological investigation

3.9.1.1. Evidence of PCOS induction from histopathology

Ovaries from rats with PCOS and control group stained with H&E. Ovaries from PCOS group demonstrated that the ovarian follicles had changed into a cystic formation **(Fig. 8)**.

3.9.1.2. Histopathology of the kidney

Kidney sections of control group demonstrated normal architecture. Compared to control group, kidney sections from PCOS group revealed atrophy, decreased glomerular cellular density, and marked deformity of renal corpuscles. The renal tubules showed degenerated lining cells with moderate chronic inflammatory cell infiltrate and dilated luminal cavities.

When compared with PCOS group, kidney tissue of DADS pre-treatment group showed obvious preservation of normal histological structure of the renal cortex and medulla. While kidney tissue of DADS post-treatment group showed renovation of glomeruli, tubules, and cortical renal corpuscles' normal structure with some remaining tubules presented mild degenerative alterations **(Fig. 9)**.

3.9.2. Immunohistochemical Staining

3.9.2.1. Effect of DADS on the immunohistochemical expression of Bcl2 in rat kidney

Kidneys from control rats demonstrate marked Bcl2 cytoplasmic expression in the cortical glomerular capillaries. Kidneys from PCOS rats displayed diminished cytoplasmic expression of Bcl2 in cortical glomerular capillaries in contrast to the control group. PCOS rats with DADS pre-treatment showed a notable rise in the expression of Bcl2 in the renal cortex and medulla contrasted with PCOS rats. Alternatively, DADS therapy after induction of PCOS demonstrates a moderate expression of Bcl2 in the renal cortex compared to PCOS rats **(Fig. 10)**.

3.9.2.2. Effect of DADS on the immunohistochemical expression of caspase-3 in rat kidney

Kidneys from control rats demonstrate negative expression of caspase-3. Kidneys from PCOS rats exhibited moderate nuclear expression of caspase-3 in cortical glomerular capillaries and renal tubules. PCOS rats pretreated with DADS demonstrate a negative expression of caspase-3. On the other hand, treatment with DADS after induction of PCOS demonstrates mild caspase-3 expression in the cortical glomerular capillaries and renal tubules **(Fig. 11)**.

4. Discussion

The complicated pathology of PCOS represents a major health and socioeconomic burden. PCOS plays a significant role in the emergence of CKD **(Du et al., 2023)**. There are limited therapeutic approaches for managing the metabolic complications of PCOS. The tendency to use natural antioxidants and anti-inflammatory agents to regulate metabolism and hyperlipidemia has increased because of drugs side effects **(Ma and Tan, 2017)**. Natural antioxidants and anti-inflammatory agents present a novel and safe approach for better control of the disease. This study used DADS to explore its potential effect on kidney disease associated with PCOS.

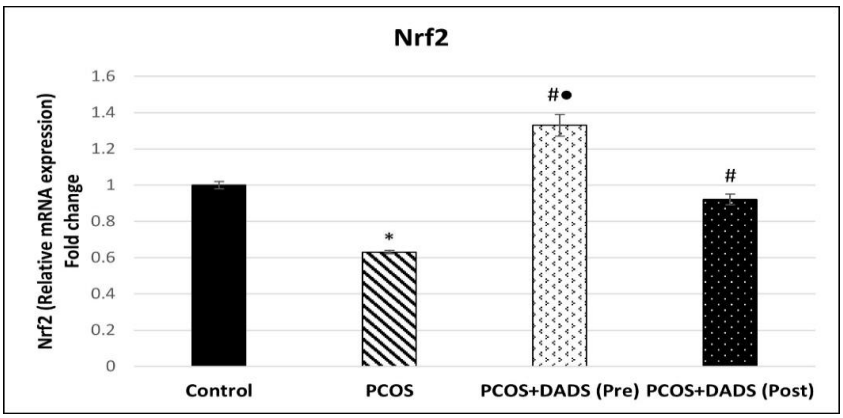

Fig. 5. Effect of DADS (50 mg kg^{-1} day^{-1}, p.o.) on the expression of renal gene Nrf2 in LET (1 mg kg^{-1} day^{-1}, p.o.)-induced PCOS. Data are displayed as mean ± SE (n=8). PCOS=Polycystic ovary syndrome, DADS=Diallyl disulfide, Nrf2= Nuclear factor erythroid 2-related factor 2. * p<0.05 contrasted with control group, # p<0.05 contrasted with PCOS group, ● p<0.05 contrasted with DADS (post) group.

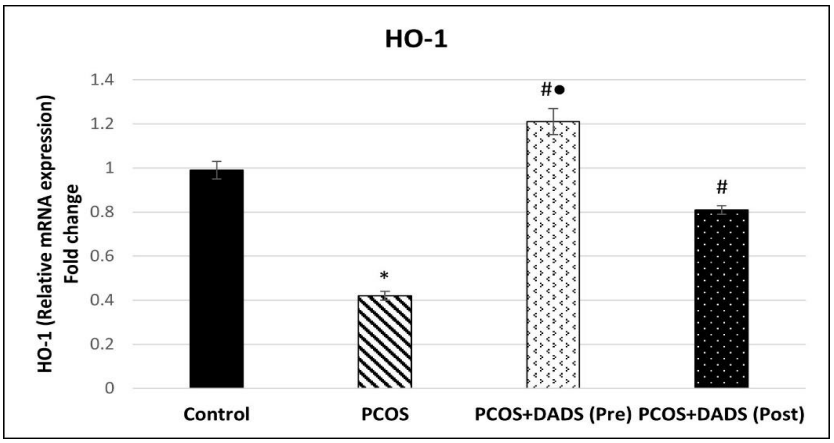

Fig. 6. Effect of DADS (50 mg kg^{-1} day^{-1}, p.o.) on the expression of renal gene HO-1 in LET (1 mg kg^{-1} day^{-1}, p.o.)-induced PCOS. Data are displayed as mean ± SE (n=8). PCOS=Polycystic ovary syndrome, DADS=Diallyl disulfide, HO-1= Heme oxygenase-1. * p<0.05 contrasted with control group, # p<0.05 contrasted with PCOS group, ● p<0.05 contrasted with DADS (post) group.

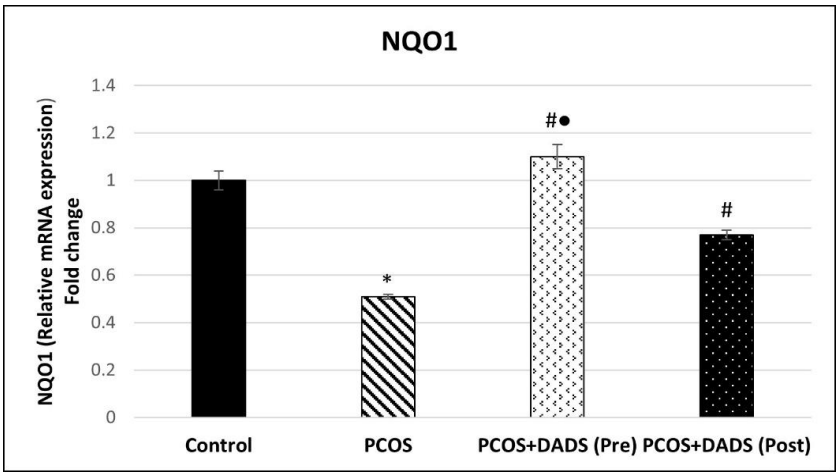

Fig. 7. Effect of DADS (50 mg kg^{-1} day^{-1}, p.o.) on the expression of renal gene NQO1 in LET (1 mg kg^{-1} day^{-1}, p.o.)-induced PCOS. Data are displayed as mean ± SE (n=8). PCOS=Polycystic ovary syndrome, DADS=Diallyl disulfide, NQO1= NADPH quinone oxidoreductase 1. * p<0.05 contrasted with control group, # p<0.05 contrasted with PCOS group, ● p<0.05 contrasted with DADS (post) group.

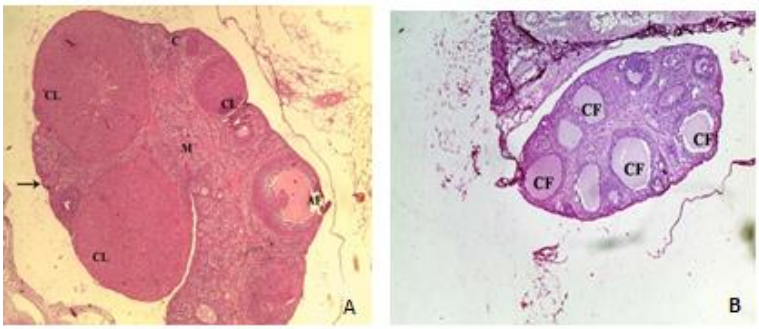

Fig. 8. H&E photos showing: (A, x40) Ovary of the control group revealed normal ovarian follicles, **black arrow:** Tunica albuginea, **C:** Cortex, **M:** Medulla, **CL:** Corpus luteum, **AF**: Antral follicle. **(B, x40)** Ovary of the PCOS group showed the change of follicles into cystic formations compared to normal ovary, **CF**: Cystic follicle.

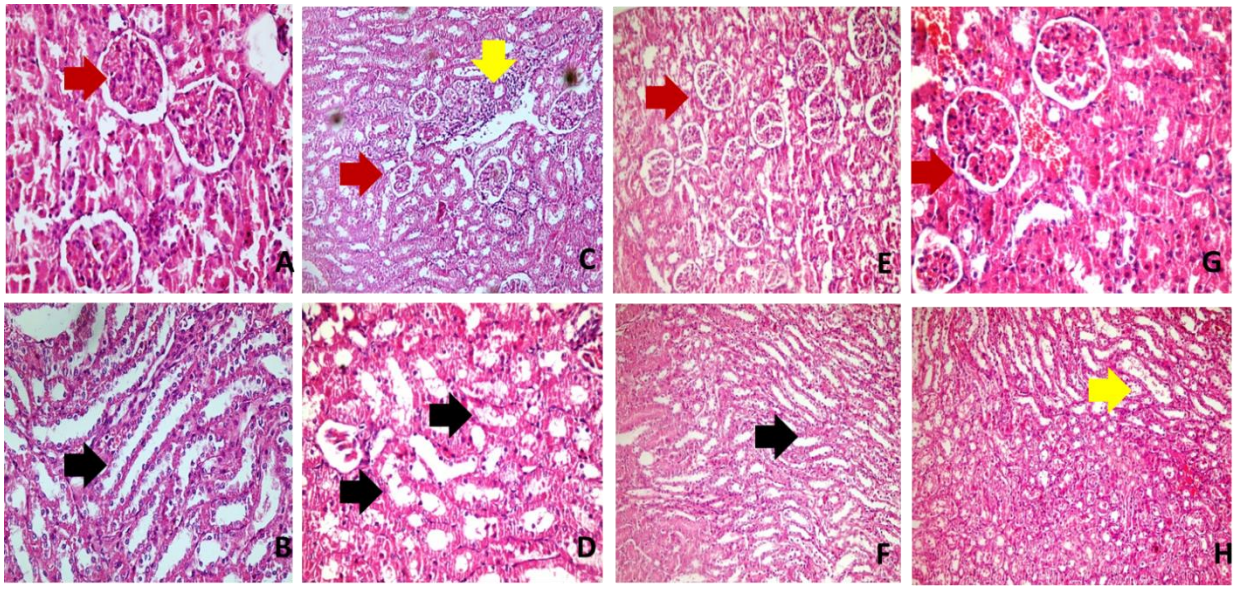

Fig. 9. H&E images demonstrating how DADS medication and PCOS affect the rat kidney's histology. (A, 400x&B, 200x) The control images display an average cell density and the usual architecture of cortical renal corpuscles and glomeruli (red arrow). The high cuboidal lining epithelium of the renal tubules appears normal (black arrow). **(C&D, 200x)** Images of PCOS demonstrate renal corpuscle malformation, severe atrophy, decreased glomerular cellular density (red arrow), and infiltration by chronic inflammatory cells (yellow arrow). There are deteriorated lining cells and dilated lumina in the kidney tubules (black arrows). **(E&F 200x)** DADS pre-treatment group, pictures demonstrate notable retention of the normal cortical (red arrow) and medullary (black arrow) histological architecture. **(G, 400x&H, 200x)** DADS post-treatment group, images demonstrate the usual cortical renal corpuscle, glomerulus (red arrow), and tubule structures restored, except for a small number of remaining tubules with minor degenerative alterations (yellow arrow).

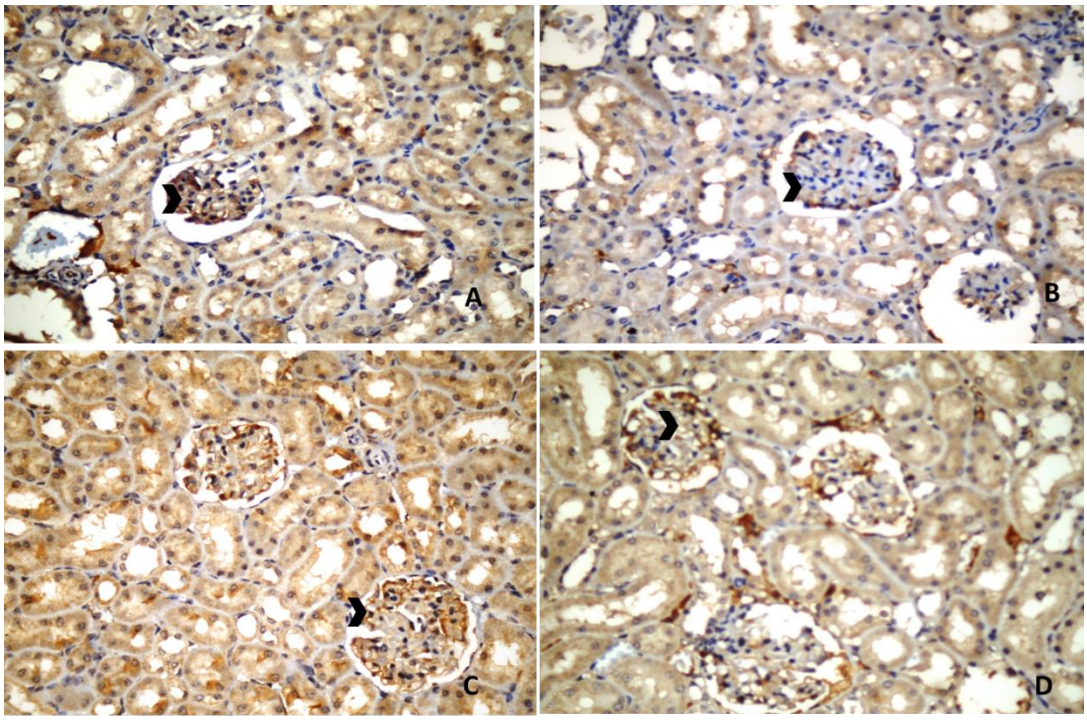

Fig. 10: Immunohistochemical expression of Bcl2 in rat kidney. (A, 400x) Control photo shows marked cytoplasmic expression of Bcl2 in the cortical glomerular capillaries (Head arrow). **(B, 400x)** PCOS photo shows weak Bcl2 staining (Head arrow). **(C, 400x)** DADS pre-treatment group photo shows a marked increase in the expression of Bcl2 (Head arrow). **(D, 400x)** DADS post-treatment group photo shows moderate expression of Bcl2 (Head arrow).

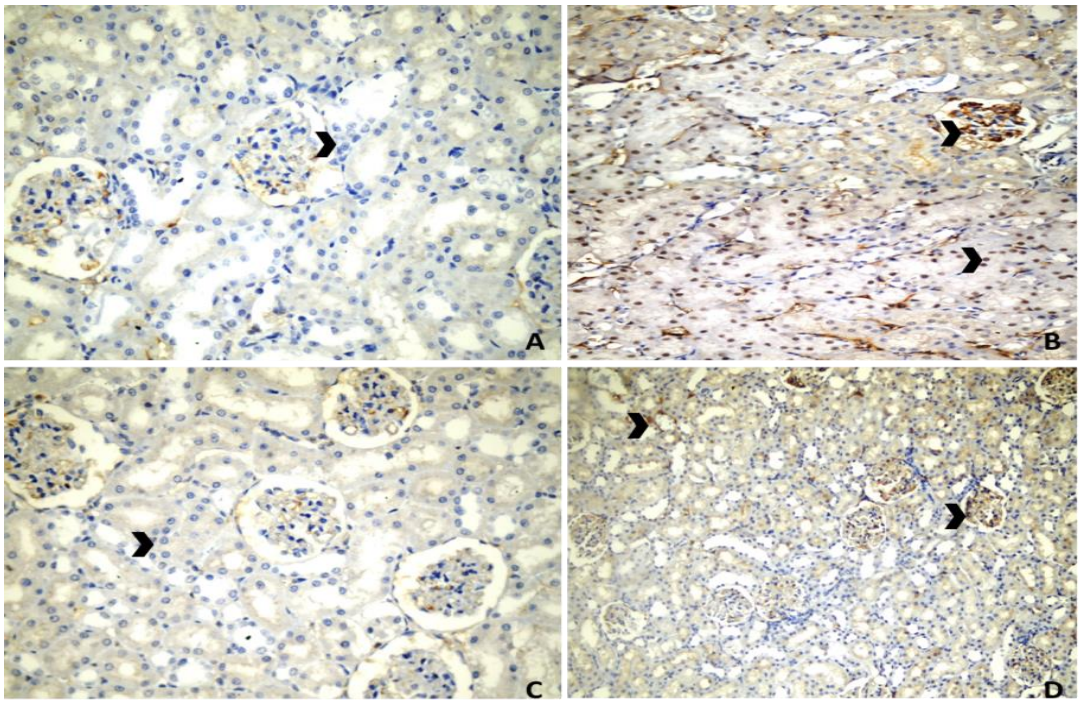

Fig. 11. Immunohistochemical expression of caspase-3 in rat kidney. (A, 400x) Control photo shows negative expression of caspase-3 in the cortical glomerular capillaries and renal tubules (Head arrow). **(B, 200x)** PCOS photo shows moderate nuclear expression of caspase-3 in the cortical glomerular capillaries and renal tubules (Head arrows). **(C, 400x)** DADS pre-treatment group photo shows negative expression of caspase-3 (Head arrow). **(D, 200x)** DADS post-treatment group photo shows mild expression of caspase-3 (Head arrows).

In PCOS rat model, our study demonstrated through biochemical and histological evidence that PCOS is linked to impaired renal function. The results demonstrated increased body weight, hyperinsulinemia, hyperglycemia, hyperandrogenism, dyslipidemia, increased oxidative stress markers (MDA and NOX4), decreased antioxidant defense (SOD, GST, and PON1), and elevated serum levels of urea and creatinine. PCOS group also showed an increased level of pro-inflammatory mediators (STAT1, NF-κB, TNFα, and IL6), decreased level of anti-inflammatory mediator IL10, decreased expression of Nrf2, HO-1, and NQO1 genes and apoptosis as indicated by immunoreactivity of renal tissue with decreased Bcl2 and increased caspase-3 antibodies. Our results are in agreement with earlier studies **(Mancini et al., 2021; Bashir and Olaniyi, 2023; Ji et al., 2023; Ye et al., 2023)**. In comparison to the untreated PCOS group, concurrent DADS administration attenuated these abnormalities in the kidney of PCOS rats.

A characteristic manifestation of metabolic-driven kidney disease is impaired glucose tolerance resulting from insulin resistance **(Habib, 2018)**. The current research demonstrated dysregulation in glucose level as evidenced by elevated glucose and insulin level in PCOS group in comparison to control group. Fortunately, it was determined that DADS supplementation had metabolic advantages, illustrated by the marked reduction in hyperglycemia, hyperinsulinemia, and body weight, and this is in line with **(Tsuzuki et al., 2024)**. DADS improved hypercholesterolemia as shown in treated groups compared with untreated PCOS group and this is in harmony with previous study in which DADS inhibits diet-induced hypercholesterolemia **(Kim and Kim, 2023)**.

Additionally, elevated testosterone level in PCOS may cause kidney damage **(Peng et al., 2019)**. Treatment with DADS significantly decreases testosterone level and inhibits testosterone-induced oxidative stress, and this is in harmony with earlier observation **(Prasad et al., 2006)**. Decreased testosterone level by DADS was also accompanied by enhancement in glucose control and a corresponding rise in insulin sensitivity, so reducing extra body weight and dyslipidemia. These findings supported the anti-metabolic advantages of DADS in metabolic-linked pathologies and clearly evidenced the role of DADS against hyperglycemia-mediated oxidative damage **(Huang et al., 2013; Wu et al., 2021)**.

The main outcome of the present work shows that DADS reduced kidney oxidative stress and inflammation in a rat model of PCOS. Reduced antioxidant defense resulted in elevated lipid peroxidation (MDA) as detected in PCOS animals with disproportionate concentrations of antioxidants (SOD, GST, and PON1) and oxidants (NOX4) leads to oxidative stress in the kidney tissue. Cellular structures are vulnerable to damage due to oxidative stress; inflammation is the body's essential immune response defense mechanism against an injury, infection, or stimulus. Nevertheless, chronic inflammation stimulates the emergence of many diseases and triggers immune deficiency **(Gupta et al., 2018)**. This activates the STAT1/NF-κB inflammatory transcription factor-signaling pathway. Stimulation of the NF-κB dependent mechanism thus releases pro-inflammatory cytokines (TNFα and IL6). These observations suggest that PCOS is associated with renal inflammation. The association is characterized by increased STAT1/ NF-κB, TNFα, and IL6 and decreased IL10. Increased caspase-3 and decreased Bcl2 expression in cortical glomerular capillaries and renal tubules in PCOS animals and declining renal function with corresponding increases in serum creatinine and urea all indicate that the renal inflammation worsens to cellular apoptosis.

However, DADS administration to PCOS animals significantly reduced inflammation by a decrease in STAT1, NF-κB, TNFα, and IL6 and elevated anti-inflammatory mediator IL10. These consequently minimize cellular apoptosis/injury, as shown with a significant decrease in caspase-3 and a marked increase in Bcl2 expression in cortical glomerular capillaries and renal tubules. Also, restores renal function as it improves serum creatinine and urea in DADS group compared with PCOS group. This demonstrates how DADS prevents and treats renal damage in a PCOS model by having anti-inflammatory and anti-apoptotic properties. The previously mentioned results of DADS are comparable to past research that showed the anti-inflammatory and anti-apoptotic effects of DADS **(Ko et al., 2017; Sharma et al., 2021; Hassanein et al., 2021)** in non-metabolic-driven pathologies.

Interestingly, the transcription factor Nrf2 has been established to be the primary molecule controlling the cellular antioxidant response. Under baseline circumstances, Nrf2 forms a bond to Keap-1. After activation, it moves to the nucleus and attaches

itself to the antioxidant response element **(Zhang et al., 2012)**. This process triggers the production of downstream antioxidants, which is essential for preserving the balance between oxidants and antioxidants **(Uruno and Motohashi, 2011)**. In this study, we found that in PCOS group there was more GST, SOD, and PON1 depletion than in control group, suggesting the critical role of oxidative stress in amplifying the susceptibility of PCOS-induced kidney injury. Our results showed significant elevation in the levels of oxidative stress markers, particularly NOX4 and MDA in PCOS group. DADS supplementation prevents the decline in Nrf2 and ameliorates the progression of kidney injury. In the current study, DADS could induce NQO-1 and HO-1 gene expressions through Nrf2 activation and increased tissue SOD, GST, and PON1 that may account for the effect of DADS against kidney injury associated with PCOS. In addition to lessening the severity of the disease, DADS treatment demonstrated NOX4 and MDA suppression actions. These data demonstrate the usefulness of DADS in preventing renal tissue damage caused by oxidative stress. In harmony with the present finding, DADS has been formerly reported to have renal protective effects in previous studies, acetaminophen **(Ko et al., 2017)**, methotrexate **(Hassanein et al., 2021)**, and glycerol **(Sharma et al., 2021)**.

5. Conclusion

Collectively, the findings imply that DADS improves renal dysfunction in LET-induced PCOS by diminishing androgen excess, enhancing antioxidant, anti-inflammatory, and anti-apoptotic activities through targeting Nrf2/HO-1, STAT1/ NF-κB signaling and modification of caspase3 and Bcl2 expression respectively. This study offered proof of the advantages of DADS in amelioration of kidney damage related to PCOS. In addition, this study recommends the use of DADS as an adjuvant therapy to protect and treat kidney injury linked to PCOS.

Conflicts of Interest

The authors declare no conflict of interest.

References

Azziz R, Carmina E, Chen Z, Dunaif A, Laven JS, Legro RS, Lizneva D, Natterson-Horowtiz B, Teede HJ, Yildiz BO, 2016. Polycystic ovary syndrome. Nat Rev Dis Primers, 2:16057.

Bashir AM, Olaniyi KS, 2023. Butyrate alleviates renal inflammation and fibrosis in a rat model of polycystic ovarian syndrome by suppression of SDF-1. BMC Pharmacol Toxicol, 24(1):48.

Behboudi-Gandevani S, Amiri M, Cheraghi L, Amanollahi Soudmand S, Azizi F, Ramezani Tehrani F, 2020. The risk of chronic kidney disease among women with polycystic ovary syndrome: A long-term population-based cohort study. Clin Endocrinol (Oxf), 93(5):590-597.

Chadban S, Howell M, Twigg S, Thomas M, Jerums G, Cass A, Campbell D, Nicholls K, Tong A, Mangos G, Stack A, MacIsaac RJ, Girgis S, Colagiuri R, Colagiuri S, Craig J; CARI, 2010. The CARI guidelines. Assessment of kidney function in type 2 diabetes. Nephrology (Carlton), 15(Suppl 1): S146-161.

Cooney LG, Dokras A, 2018. Beyond fertility: polycystic ovary syndrome and long-term health. Fertil Steril, 110(5):794-809.

Cooney LG, Lee I, Sammel MD, Dokras A, 2017. High prevalence of moderate and severe depressive and anxiety symptoms in polycystic ovary syndrome: a systematic review and meta-analysis. Hum Reprod, 32(5):1075-1091.

Du Y, Li F, Li S, Ding L, Liu M, 2023. Causal relationship between polycystic ovary syndrome and chronic kidney disease: A Mendelian randomization study. Front Endocrinol (Lausanne), 14:1120119.

Escobar-Morreale HF, 2018. Polycystic ovary syndrome: definition, aetiology, diagnosis and treatment. Nat Rev Endocrinol, 14(5):270-284.

Friedewald WT, Levy RI, Fredrickson DS, 1972. Estimation of the concentration of low-density lipoprotein cholesterol in plasma, without use of the preparative ultracentrifuge. Clin Chem, 18(6):499-502.

Goodarzi MO, Dumesic DA, Chazenbalk G, Azziz R, 2011. Polycystic ovary syndrome: etiology, pathogenesis and diagnosis. Nat Rev Endocrinol, 7(4):219-231.

Gupta SC, Kunnumakkara AB, Aggarwal S, Aggarwal BB, 2018. Inflammation, a Double-Edge Sword for Cancer and Other Age-Related Diseases. Front Immunol, 9:2160.

Habib SL, 2018. Kidney atrophy vs hypertrophy in diabetes: which cells are involved? Cell Cycle,

17(14):1683-1687.

Habig WH, Pabst MJ, Jakoby WB, 1974. Glutathione S-transferases. The first enzymatic step in mercapturic acid formation. J Biol Chem, 249(22):7130-7139.

Hassanein EHM, Mohamed WR, Khalaf MM, Shalkami AS, Sayed AM, Hemeida RAM, 2021. Diallyl disulfide ameliorates methotrexate-induced nephropathy in rats: Molecular studies and network pharmacology analysis. J Food Biochem, 45(6): e13765.

Huang YT, Yao CH, Way CL, Lee KW, Tsai CY, Ou HC, Kuo WW, 2013. Diallyl trisulfide and diallyl disulfide ameliorate cardiac dysfunction by suppressing apoptotic and enhancing survival pathways in experimental diabetic rats. J Appl Physiol (1985), 114(3):402-10.

Ji R, Jia F, Chen X, Gao Y, Yang J, 2023. Carnosol inhibits KGN cells oxidative stress and apoptosis and attenuates polycystic ovary syndrome phenotypes in mice through Keap1-mediated Nrf2/HO-1 activation. Phytother Res, 37(4):1405-1421.

Kim HJ, Kim M, 2023. Diallyl disulfide alleviates hypercholesterolemia induced by a western diet by suppressing endoplasmic reticulum stress in apolipoprotein E-deficient mice. BMC Complement Med Ther, 23(1):141.

Ko JW, Shin JY, Kim JW, Park SH, Shin NR, Lee IC, Shin IS, Moon C, Kim SH, Kim SH, Kim JC, 2017. Protective effects of diallyl disulfide against acetaminophen-induced nephrotoxicity: A possible role of CYP2E1 and NF-κB. Food Chem Toxicol, 102:156-165.

Lee IC, Kim SH, Baek HS, Moon C, Kang SS, Kim SH, Kim YB, Shin IS, Kim JC, 2014. The involvement of Nrf2 in the protective effects of diallyl disulfide on carbon tetrachloride-induced hepatic oxidative damage and inflammatory response in rats. Food Chem Toxicol, 63:174-185.

Livak KJ, Schmittgen TD, 2001. Analysis of relative gene expression data using real-time quantitative PCR and the 2(-Delta Delta C(T)) Method. Methods, 25(4):402-408.

Ma QW, Tan Y, 2017. Effectiveness of co-treatment with traditional Chinese medicine and letrozole for polycystic ovary syndrome: a meta-analysis. J Integr Med, 15(2):95-101.

Mancini A, Bruno C, Vergani E, d'Abate C, Giacchi E, Silvestrini A, 2021. Oxidative Stress and Low-Grade Inflammation in Polycystic Ovary Syndrome: Controversies and New Insights. Int J Mol Sci, 22(4):1667.

Nigam SK, Bush KT, 2019. Uraemic syndrome of chronic kidney disease: altered remote sensing and signalling. Nat Rev Nephrol, 15(5):301-316.

Nishikimi M, Appaji N and Yagi K, 1972. The occurrence of superoxide anion in the reaction of reduced phenazine methosulfate and molecular oxygen. Biochem Biophys Res Commun, 46(2):849-854.

Ohkawa H, Ohishi N, Yagi K, 1979. “Assay for lipid peroxides in animal tissues by thiobarbituric acid reaction”. Anal Biochem, 95(2):351-358.

Olaniyi KS, Oniyide AA, Adeyanju OA, Ojulari LS, Omoaghe AO, Olaiya OE, 2021. Low dose spironolactone-mediated androgen-adiponectin modulation alleviates endocrine-metabolic disturbances in letrozole-induced PCOS. Toxicol Appl Pharmacol, 411:115381.

Patil CN, Racusen LC, Reckelhoff JF, 2017. Consequences of advanced aging on renal function in chronic hyperandrogenemic female rat model: implications for aging women with polycystic ovary syndrome. Physiol Rep, 5(20): e13461.

Peng Y, Fang Z, Liu M, Wang Z, Li L, Ming S, Lu C, Dong H, Zhang W, Wang Q, Shen R, Xie F, Zhang W, Yang C, Gao X, Sun Y, 2019. Testosterone induces renal tubular epithelial cell death through the HIF-1α/BNIP3 pathway. J Transl Med, 17(1):62.

Piccoli GB, Alrukhaimi M, Liu ZH, Zakharova E, Levin A; World Kidney Day Steering Committee, 2018. Women and kidney disease: reflections on World Kidney Day 2018: Kidney Health and Women's Health: a case for optimizing outcomes for present and future generations. Nephrol Dial Transplant, 33(2):189-193.

Prasad S, Kalra N, Shukla Y, 2006. Modulatory effects of diallyl sulfide against testosterone-induced oxidative stress in Swiss albino mice. Asian J Androl, 8(6):719-723.

Sharma AK, Kaur A, Kaur J, Kaur G, Chawla A, Khanna M, Kaur H, Kaur H, Kaur T, Singh AP, 2021. Ameliorative Role of Diallyl Disulfide Against Glycerol-induced Nephrotoxicity in Rats. J Pharm Bioallied Sci, 13(1):129-135.

Somade OT, Adedokun AH, Adeleke IK, Taiwo MA, Oyeniran MO, 2019. Diallyl disulfide, a garlic-rich compound ameliorates

trichloromethane-induced renal oxidative stress, NFkB activation and apoptosis in rats. Clin Nutr Exp, 23:44-59.

Tsuzuki T, Negishi T, Yukawa K, 2024. Effects of diallyl disulfide administration on insulin resistance in high-fat diet-fed mice. Nutrition, 118:112292.

Uruno A, Motohashi H, 2011. The Keap1-Nrf2 system as an in vivo sensor for electrophiles. Nitric Oxide, 25(2):153-160.

Wu YR, Li L, Sun XC, Wang J, Ma CY, Zhang Y, Qu HL, Xu RX, Li JJ, 2021. Diallyl disulfide improves lipid metabolism by inhibiting PCSK9 expression and increasing LDL uptake via PI3K/Akt-SREBP2 pathway in HepG2 cells. Nutr Metab Cardiovasc Dis, 31(1):322-332.

Ye HY, Song YL, Ye WT, Xiong CX, Li JM, Miao JH, Shen WW, Li XL, Zhou LL, 2023. Serum granulosa cell-derived TNF-α promotes inflammation and apoptosis of renal tubular cells and PCOS-related kidney injury through NF-κB signaling. Acta Pharmacol Sin, 44(12):2432-2444.

Zhang H, Liu H, Davies KJ, Sioutas C, Finch CE, Morgan TE, Forman HJ, 2012. Nrf2-regulated phase II enzymes are induced by chronic ambient nanoparticle exposure in young mice with age-related impairments. Free Radic Biol Med, 52(9):2038-2046.